To be submitted to ...
DRAFT DRAFT DRAFT DRAFT October 26, 2008

A synchrobetatron condition on the grazing function g for efficient crystal collimation

S. Peggs (BNL) and V. Previtali (CERN)

1 Introduction

The total horizontal displacement x_T of a particle as it passes a crystal is the sum of its betatron and synchrotron displacements[1],

$$x_T \;=\; x_\beta + x_s \tag{1}$$

where the betatron displacement and angle oscillate according to

$$\begin{aligned} x_\beta &= a_x \sin(\phi_x) && (2)\\ x'_\beta &= \frac{a_x}{\beta}\,(\cos(\phi_x) - \alpha\sin(\phi_x)) && (3) \end{aligned}$$

Here β and α are horizontal twiss functions at the crystal, a_x is the betatron amplitude, and the betatron phase advances with turn number t according to

$$\phi_x \;=\; 2\pi Q_x t + \phi_{x0}, \tag{4}$$

Similarly, the synchrotron displacement and angle are

$$\begin{aligned} x_s &= \eta\,\delta && (5)\\ x'_s &= \eta'\,\delta && (6) \end{aligned}$$

where $\delta = \Delta p/p$ is the relative momentum offset, which performs synchrotron oscillations according to

$$\begin{aligned} \delta &= a_s \sin(\phi_s) && (7)\\ &= a_s \sin(2\pi Q_s t + \phi_{s0}) && (8) \end{aligned}$$

Here η and η' (dispersion and dispersion-prime) are optical quantities at the crystal, complementing β and α. Only one of the four, β, is positive-definite. The total angle x'_T of a particle is thus written in general as

$$x'_T \;=\; \frac{a_x}{\beta}\,(\cos(\phi_x) - \alpha\sin(\phi_x)) \;+\; \eta' a_s \sin(\phi_s) \tag{9}$$

1.1 The grazing function

Consider a test particle that just grazes the edge of a crystal displaced by x_c when its betatron and synchrotron displacements are simultaneously at their extrema – either maxima or minima – such that

$$a_x + |\eta|\, a_s \;=\; |x_c| \tag{10}$$

This equation correlates the betatron and synchrotron amplitudes of the set of grazing particles, since it is trivially rewritten as

$$a_x \;=\; |x_c| - |\eta|\, a_s \tag{11}$$

Simultaneous betatron and synchrotron oscillation extrema are achieved at phases

$$\phi_x \;=\; \mathrm{sgn}(x_c) \quad \pi/2 \tag{12}$$

$$\phi_s \;=\; \mathrm{sgn}(x_c)\,\mathrm{sgn}(\eta) \quad \pi/2 \tag{13}$$

where the possibilities of negative crystal displacement x_c and negative dispersion η are explicitly taken into account.

The *grazing angle* – the total angle of grazing particles – is found by substituting these phases into equation 9 and by using equation 11 to eliminate a_x. It is

$$x'_G \;=\; -\frac{\alpha}{\beta}x_c \;+\; \mathrm{sgn}(x_c)\,\mathrm{sgn}(\eta)\left(\frac{\alpha}{\beta}\eta \;+\; \eta'\right)\, a_s \tag{14}$$

Thus the grazing angle depends linearly on the synchrotron amplitude a_s according to

$$x'_G \;=\; -\frac{\alpha}{\beta}x_c \;+\; \mathrm{sgn}(x_c)\,\mathrm{sgn}(\eta)\; g\, a_s \tag{15}$$

where the linear slope of grazing angle with respect to synchrotron amplitude is

$$\frac{dx'_G}{da_s} \;=\; \mathrm{sgn}(x_c)\,\mathrm{sgn}(\eta)\, g \tag{16}$$

The *grazing function* g that enters these equations is an optical quantity defined as

$$g \;\equiv\; \left(\frac{\alpha}{\beta}\eta \;+\; \eta'\right) \tag{17}$$

Any such linear dependence of the grazing angle on the synchrotron amplitude is undesirable, since it may cause particles with some synchrotron amplitudes to fall outside the limited angular acceptance that a crystal has for channeling, and also for volume reflection. The rigorous synchrobetatron condition for constant grazing angle is

$$g \;=\; 0 \tag{18}$$

This exact condition has not been met (or will not be met) in realistic implementations in RHIC, SPS, Tevatron and LHC, not only because of the presence of optical errors, but also because ideal crystal locations have not (so far) been available by design.

2 RHIC, SPS, Tevatron & LHC

How close is it necessary to get to the rigorous condition of equation 18? What are the implications for RHIC, SPS, Tevatron and LHC?

Table 1 shows that realistic crystal implementations have grazing functions – either positive or negative – with an order of magnitude of 0.003. Inspection of the 4 pairs of η' and g values in the table shows a strong cancellation between the two terms that comprise g in equation 17. This is due to the intimate connection between the grazing function and the normalized dispersion, which is discussed further, below.

	α	β [m]	η [m]	η' [10^{-3}]	g [10^{-3}]	E [TeV]	σ_p/p [10^{-3}]	σ'_G [μ rad]
RHIC	-26.5	1155.0	-0.864	-16.2	3.6	0.10	0.50	1.81
SPS	-2.21	96.1	-0.880	-19.0	1.2	0.12	0.40	0.48
Tevatron	-0.425	67.5	1.925	15.0	2.9	0.98	0.14	0.41
LHC	1.94	137.6	0.559	-8.9	-1.0	0.45	0.31	0.31
						7.0	0.11	0.11

Table 1: Nominal optics and grazing function values for accelerators involved in crystal collimation experiments, or in planning.

2.1 Grazing angle spread

The RMS spread of the grazing angle for incident particles with an RMS momentum spread of σ_p/p is

$$\sigma'_G = |g| \left(\frac{\sigma_p}{p} \right) \tag{19}$$

and is recorded for the 4 accelerators in the last column of table 1. The most probable synchrotron amplitude in a bunch is about 1 σ_p/p, although many particles have a synchrotron amplitude close to zero. Typically the crystal displacement $|x_c|$ is several times the beam size, and so grazing particles preferentially have betatron and/or synchrotron amplitudes much larger than 1, measured in units of RMS beam size. In some situations (like RHIC[2]) the synchrotron amplitude spectrum is truncated at a few σ_p/p by the edge of the RF bucket. In general (without descending into implementation-specific detail) all particles with a range of synchrotron amplitudes

$$0 \ < \ a_s \ < \ n_{max} \left(\frac{\sigma_p}{p} \right) \tag{20}$$

must fall within the crystal acceptance angle σ'_A, where $n_{max} \geq 3$, in order for (almost) all particles to be efficiently collimated. It is therefore necessary that

$$n_{max}\,\sigma'_G \;<\; \sigma'_A \tag{21}$$

Thus the exact synchrobetatron condition can be relaxed to the more practical result

$$|g| \;<\; \frac{\sigma'_A}{n_{max}\,(\sigma_p/p)} \tag{22}$$

2.2 Crystal angular acceptance

The value of the acceptance angle varies widely, depending on implementation-specific details such as the geometry of the crystal, the beam species and energy, and the mode of crystal operation. Roughly speaking, the order of magnitude acceptance angle for protons is

$$\sigma'_A\ [\mu\text{rad}] \sim 2 \quad \text{channeling at 7 TeV} \tag{23}$$
$$\sim 10 \quad \text{channeling at 0.1 TeV} \tag{24}$$
$$\sim 100 \quad \text{volume reflection at any energy} \tag{25}$$

The volume reflection acceptance angle is simply the crystal bend angle, and so is superficially independent of particle energy. In contrast, the channeling acceptance angle decreases significantly with increasing energy. Because the maximum permissible grazing function given by equation 22 decreases at higher energies for channeling, volume reflection appears to become more favored at higher energies, at least in some scenarios.

2.3 RHIC

Figure 1 shows the RHIC design conditions for the crystal collimation experiment reported at length by Fliller [2], and corresponding to the values reported in table 1 [3]. The figure and the table show that the grazing angle varied by about 5.4 μrad over synchrotron amplitudes from zero to 3 σ_p/p, at the edge of the RF bucket [4]. This is a range of about half of the channeling acceptance angle [5]. It could be one of the root causes of the relatively poor collimation efficiency that was observed in practice.

In addition to the collision optics values used here (with $\beta^* = 1$ m at the nearby PHENIX experiment), Fliller also records several other design optics with larger β^* values, up to a maximum value of 10 m in injection conditions [6]. The design value of β at the crystal decreases from 1155 m to 129 m, but the grazing function only changes from 0.0036 to 0.0032.

2.4 SPS

Figure 2 shows the SPS conditions expected to be encountered in the UA9 experiment, in 2009 [7]. The grazing function value of 0.0012 is almost as small (in magnitude) as in the

LHC, and a factor of 3 smaller than in RHIC, despite the significant negative dispersion value at the crystal. Conditions are therefore predicted to be better – on this basis – than in the RHIC experiment.

2.5 Tevatron

Figure 3 shows the Tevatron design conditions assumed for the ongoing T980 experiment [8]. The separation of 10 murad contours is striking, in comparison with RHIC and SPS conditions. The RMS momentum spread $\sigma_p/p = 0.00014$ is also significantly reduced, mainly due to the significantly larger energy. Despite the relatively large grazing function value of 0.0029, the T980 experiment has an RMS grazing angle value of 0.41 μrad, to be compared with crystal acceptance values. The measured optics values that are also available for the location of the T980 crystal appear to show very different g values [8]. However, these measurements results in large error bars that span the design value of g, after the subtraction of one number from another of similar size.

2.6 LHC

Figure 4 shows the 7 TeV case for the LHC configuration currently under discussion, in which the design grazing function $g = -0.0010$ is negative, and the RMS momentum spread is only $\sigma_p/p = 0.00011$. The spread in grazing angle could still be an issue in the LHC, despite its modest value, because of the extremely stringent collimation efficiency requirements and because the crystal channeling acceptance angle is only about 2 μrad.

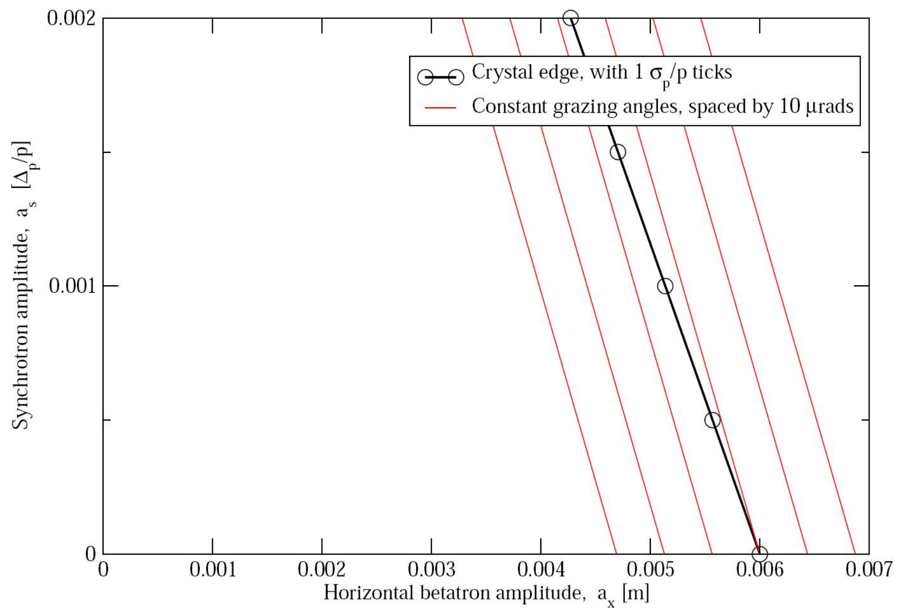

Figure 1: RHIC: as encountered in the prototype crystal collimation scheme reported at length by Fliller [2]. The grazing angle change between small circles (with synchrotron amplitudes spaced by 1 σ_p/p) is 1.81 μradians, an order of magnitude larger than in the LHC.

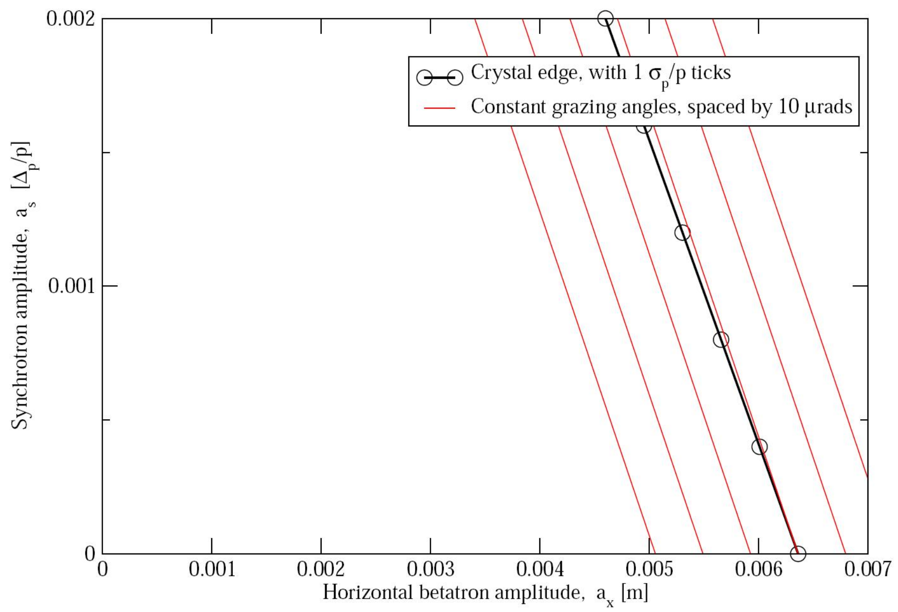

Figure 2: SPS (UA9): as expected for the UA9 experiment [7]. The small circles represent grazing particles that are spaced by 1 σ_p/p in synchrotron amplitude, with grazing angle steps of 0.48 μ radians.

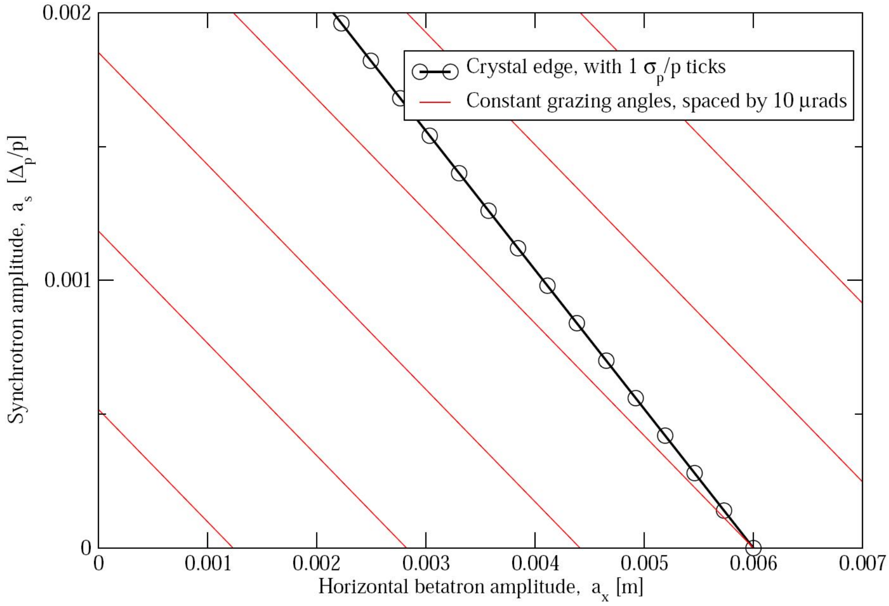

Figure 3: Tevatron (T980): as encountered in the ongoing T980 at the Tevatron. The 10 μrad contours (in red) are unusually widely spaced, and sloped, with a grazing function value of $g = 0.0029$.

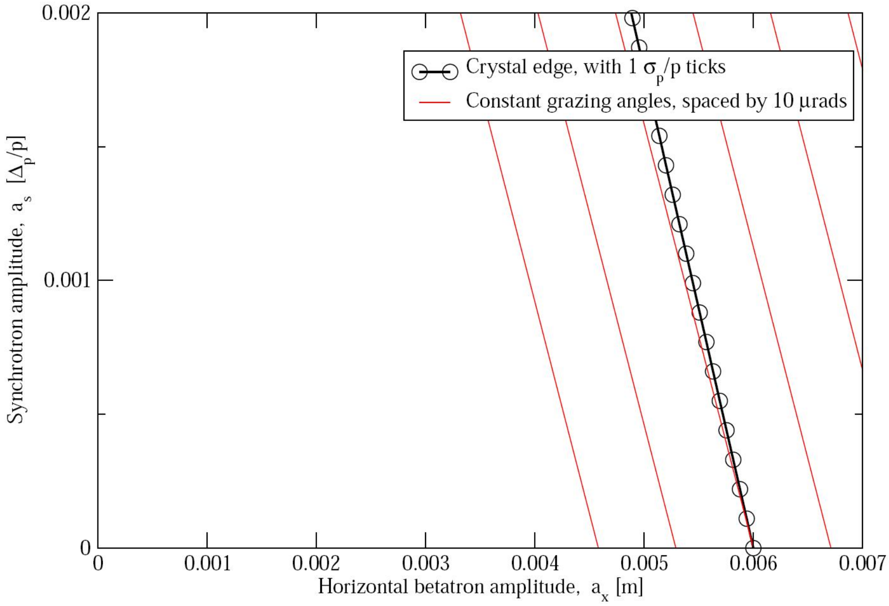

Figure 4: LHC: as discussed in a nominal collimation scheme still under consideration, shown under design conditions at 7 TeV with $\sigma_p/p = 0.00011$ and $g = -0.0010$.

3 Solving the synchrobetatron condition

The synchrobetatron condition for the ideal location of a crystal is

$$g = \frac{\alpha}{\beta}\eta + \eta' = 0 \tag{26}$$

This is a condition on the optics at the crystal, independent of the emittance and the energy spread of the beam. If it is met, the grazing angle does not depend on the synchrotron amplitude. Two particular trivial solutions are immediately obvious:

1. $\eta = \eta' = 0$: anywhere in a dispersion-free straight.
2. $\alpha = \eta' = 0$: simultaneous extrema of β and η, such as (logically) in the middle of a quadrupole at the boundary of a matched half-cell.

Fortunately, the condition can be more generally satisfied – exactly or approximately – at practical locations in magnet-free straights which are *not* dispersion free.

3.1 The general condition on normalized dispersion

The linear slope coefficient may be re-written as

$$g = \eta f' \tag{27}$$

by introducing the function

$$f = \log(\eta_N) \tag{28}$$

where the normalized dispersion is

$$\eta_N = \frac{\eta}{\sqrt{\beta}} \tag{29}$$

and by recalling that

$$\alpha = -\frac{1}{2}\beta' \tag{30}$$

The grazing function is thus revealed to be just

$$g = \sqrt{\beta}\,\eta_N' \tag{31}$$

and the rigorous general synchrobetatron condition $g = 0$ is just

$$\eta_N' = 0 \tag{32}$$

since β is positive-definite. A crystal is ideally placed at a location where normalized dispersion is at a local maximum or minimum!

4 Grazing function propagation

The differential equations describing the propagation of dispersion and the horizontal beta function are quite similar to each other:

$$\eta'' + K\eta = \frac{1}{\rho} \tag{33}$$

$$b'' + Kb = b^{-3} \tag{34}$$

where

$$b = \sqrt{\beta} \tag{35}$$

Here K represents the quadrupole field, while ρ is the bend radius of the dipole field. These equations enable the propagation of the grazing function

$$g = b\,\eta'_N = b\left(\frac{\eta'}{b} - \frac{\eta b'}{b^2}\right) = \left(\eta' - \frac{\eta b'}{b}\right) = \eta\left(\frac{\eta'}{\eta} - \frac{b'}{b}\right) \tag{36}$$

to be studied in particular cases of interest, even though a simple differential equation for g appears to be unavailable.

4.1 Across a thin dipole or quadrupole

The changes in b' and η' across a thin dipole of bend angle $\Delta\theta$ are

$$\Delta\eta' = \Delta\theta \tag{37}$$

$$\Delta b' = 0 \tag{38}$$

while b and η themselves do not change, so that the grazing function has a step of

$$\Delta g = \left(\Delta\eta' - \frac{\eta\,\Delta b'}{b}\right) = \Delta\theta \tag{39}$$

showing that g is unchanged across a thin quadrupole. Similarly, the changes in b' and η' across a thin quadrupole of integrated strength $\Delta(KL)$ are

$$\Delta\eta' = -\,\Delta(KL)\,\eta \tag{40}$$

$$\Delta b' = -\,\Delta(KL)\,b \tag{41}$$

showing that the grazing function is unchanged across a thin quadrupole, since

$$\Delta g = \eta\left(\frac{\Delta\eta'}{\eta} - \frac{\Delta b'}{b}\right) = 0 \tag{42}$$

The top plot in figure 5 confirms such propagation of g through thin magnets. In ironic contrast, there is no simple solution to propagating g through a thick drift.

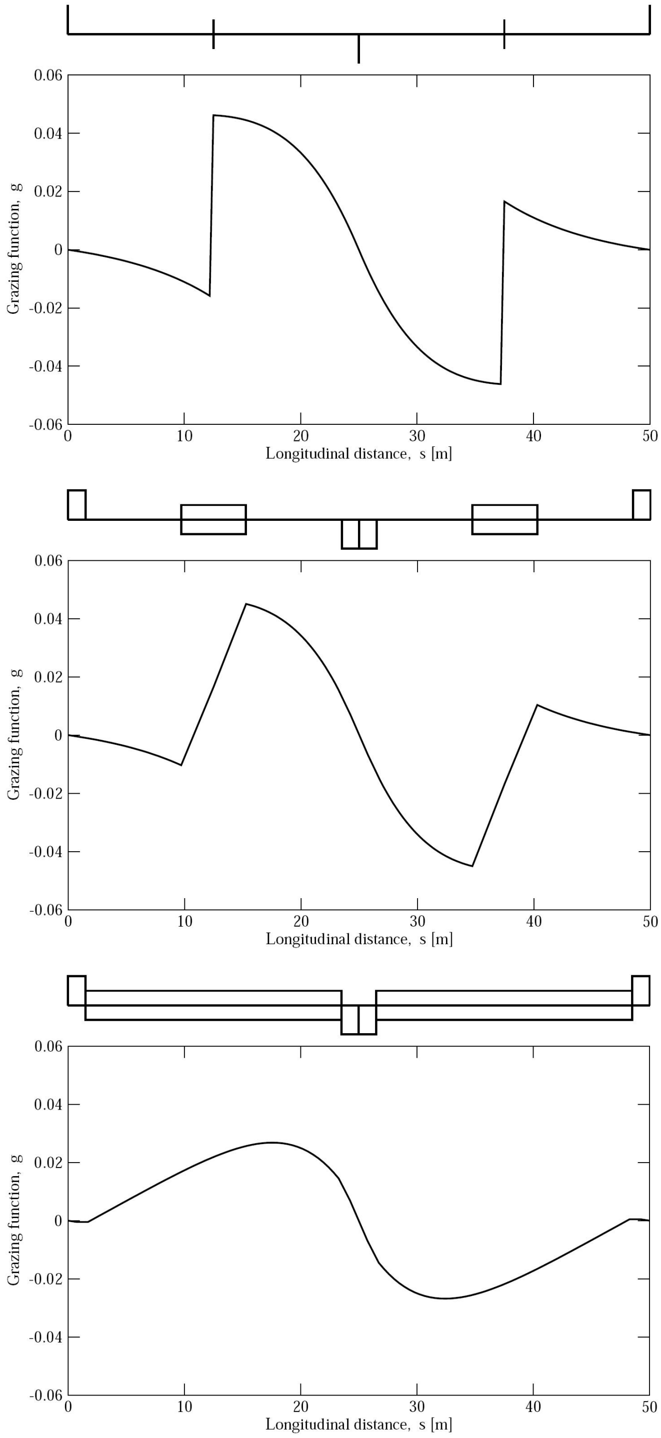

Figure 5: The grazing function in a matched FODO cell with thin quads and dipoles (top), partially filled with thick quads and dipoles (middle). and filled (bottom). In all cases the half-cell is $L = 25$ m long, with a phase advance of 90 degrees per full-cell in both planes, and with a bend angle of $\theta = \pi/50$ radians per half-cell.

4.2 Through a matched FODO half-cell

Consider a half-cell of length L with a quadrupole at each end, enclosing one or more dipoles. If this half-cell is matched ($b' = \eta' = 0$ at both ends) then g is zero at both ends, and close to zero within the quadrupoles, as illustrated in figure 5. However, η'_N and (hence) g are non-zero within the half-cell, since the normalized dispersion η_N is not exactly the same at both ends. A reasonable approximation is that η'_N evolves quadratically with s, according to

$$\eta'_N(s) \;\approx\; \frac{6\,\Delta\eta_N}{L^3}\, s(s-L) \tag{43}$$

where $\Delta\eta_N$ is the total change from end to end. The extreme values of η'_N and (hence) g are therefore expected near the middle of the half-cell, at $s = L/2$, so that

$$|g|_{max} \;\approx\; \sqrt{\beta_{mid}}\,\frac{3|\Delta\eta_N|}{2L} \tag{44}$$

The accuracy of this approximation depends on the detailed layout of the dipoles within the half-cell in the case under study.

A case of particular interest is a matched FODO half-cell containing one or more dipoles with a total bend angle of θ, centered half way along the half-cell. The maximum, minimum, and mid half-cell beta functions (assuming thin quadrupoles) are

$$\beta_F \;=\; \frac{L}{S}\left(\frac{C}{1-S}\right), \qquad \beta_D \;=\; \frac{L}{S}\left(\frac{C}{1+S}\right), \qquad \beta_{mid} \;=\; \frac{L}{S}\left(\frac{1+C^2}{2C}\right) \tag{45}$$

where

$$S \;\equiv\; \sin\phi/2, \qquad C \;\equiv\; \cos\phi/2 \tag{46}$$

and ϕ is the phase advance per full FODO cell, identical in both planes, and typically 60 or 90 degrees. Similarly, the extreme dispersion functions are

$$\eta_F \;=\; L\theta\left(\frac{2+S}{2S^2}\right), \qquad \eta_D \;=\; L\theta\left(\frac{2-S}{2S^2}\right) \tag{47}$$

Hence the normalized dispersions are

$$\eta_{N,F} \;=\; \sqrt{L}\theta\left(\frac{2+S}{2S^{3/2}C^{1/2}}\right)\sqrt{1-S}, \qquad \eta_{N,D} \;=\; \sqrt{L}\theta\left(\frac{2-S}{2S^{3/2}C^{1/2}}\right)\sqrt{1+S} \tag{48}$$

Putting all this together into equation 44 gives

$$|g|_{max} \;\approx\; \theta\,\frac{3}{4\sqrt{2}}\,\frac{\sqrt{1+C^2}}{S^2C}\,\Big((2-S)\sqrt{1+S} \;-\; (2+S)\sqrt{1-S}\Big) \tag{49}$$

In the case at hand when the phase advance per cell is 90 degrees and $C = S = 1/\sqrt{2}$ then the maximum of the grazing function is predicted to be

$$|g|_{max} \;\approx\; 0.39\;\;\theta \tag{50}$$

with no dependence on the half-cell length L.

Figure 5 shows that when $L = 25$ m and $\theta = \pi/50$, then the maximum value occurs close to the mid half-cell, with a value of $|g|_{max} = 0.0268$ that is reasonably close to the value of 0.0248 predicted by equation 50.

4.3 Scaling in a matched FODO cell

Numerical testing confirms that the maximum value of the grazing function scales with half-cell length L and with half-cell bending angle θ like

$$g_{max} \approx 0.427 \ L^0 \, \theta^1 \tag{51}$$

when the phase advance per full-cell is 90 degrees. There is no dependence on the cell length! A fair rule of thumb is that

$$g_{max} \approx \theta/2 \tag{52}$$

These results apply *only* to a matched FODO cell. The grazing function can become much larger (in absolute magnitude) when there is an unmatched dispersion (or betatron) wave, and in non-FODO locations.

Finally, insofar as the maximum dispersion function remains remarkably constant at $\eta_{max} \approx 2$ m over accelerators that span many orders of magnitude of energy γ (and ignoring an order of magnitude range of dipole fields), then

$$\theta \sim \gamma^{-1/2} \tag{53}$$

and so also

$$g_{max} \sim \gamma^{-1/2} \tag{54}$$

Fortunately the grazing function naturally decreases with increasing energy, as also does the acceptance angle for channeling in a crystal collimator.

5 Summary

The *grazing function g* parameterizes the rate of change of total angle with synchrotron amplitude for grazing particles – those that just touch the surface of the crystal when their synchrotron and betatron oscillations are simultaneously at their extreme displacements. The grazing function is a pure optics function, closely related to the slope of the normalized dispersion function, with an ideal value of $g = 0$ at the crystal.

Insofar as g is non-zero in practical implementations – for example due to optics errors or design limitations – then it should be kept small enough in magnitude so that all particles over the relevant synchrotron amplitude range remain within the crystal acceptance angle. This appears to be reasonable to achieve in practice, especially when crystals are operating in volume reflection mode, and especially at lower energies.

The grazing function is naturally small in well-matched optics with no (or small) dispersion and betatron waves, and it is identically zero in dispersionless areas. However, it is not in general necessary to make dispersion (and the dispersion slope) zero at the crystal. More important is the need to ensure the absence of significant unmatched betatron and dispersion waves, since they may increase g by an order of magnitude.

Design values for past, present and future crystal implementations in RHIC. SPS, Tevatron and LHC suggest that the natural realistic values of g are acceptably small, although they are not negligible. Planning for future crystal implementations should always include a grazing function analysis, both in design (making g zero, or small enough) and in error analysis (ensuring that g cannot become anomalously large).

6 Acknowledgments

We would like to thank R. Assmann, A. Drees, R. Fliller, E. Laface, N. Mokhov, G. Robert-Demolaize, W. Scandale, D. Still, and A. Valishev, for their support and encouragement.

References

[1] S.Shiraishi & S.Peggs, *Pattern Recognition: The Importance of Dispersion in Crystal Collimation*, BNL, C-A/AP/324, September, 2008.

[2] R.Fliller, *The Crystal Collimation System of the Relativistic Heavy Ion Collider*, Ph.D. thesis, Stony Brook University, 2004.

[3] R.Fliller, Table 1, page 4, R. Fliller thesis, ibid.

[4] A.Drees, R.Fliller, private communication, October, 2008.

[5] R.Fliller, Table 2.2, page 25, R. Fliller thesis, ibid.

[6] R.Fliller, Table 2.3, page 49, R. Fliller thesis, ibid.

[7] E. Laface, private communication, October, 2008.

[8] D.Still, A.Valishev, private communication, October, 2008.